AJNR

Gross-total Surgery of Supratentorial Low-grade Gliomas under Intraoperative MR Guidance

Jens P. Schneider, Thomas Schulz, Frank Schmidt, Jürgen Dietrich, Siegbert Lieberenz, Christos Trantakis, Volker Seifert, Steffen Kellermann, Ralf Schober, Lutz Schaffranietz, Mario Laufer and Thomas Kahn

AJNR Am J Neuroradiol 2001, 22 (1) 89-98
http://www.ajnr.org/content/22/1/89

AJNR Am J Neuroradiol 22:89–98, January 2001

Gross-total Surgery of Supratentorial Low-grade Gliomas under Intraoperative MR Guidance

Jens P. Schneider, Thomas Schulz, Frank Schmidt, Jürgen Dietrich, Siegbert Lieberenz, Christos Trantakis, Volker Seifert, Steffen Kellermann, Ralf Schober, Lutz Schaffranietz, Mario Laufer, and Thomas Kahn

BACKGROUND AND PURPOSE: **Length of survival of patients with low-grade glioma correlates with the extent of tumor resection. These tumors, however, are difficult to distinguish intraoperatively from normal brain tissue, often leading to incomplete resection. Our goal was to evaluate the effectiveness of intraoperative MR guidance in achieving gross-total resection.**

METHODS: **We studied 12 patients with low-grade glioma who underwent surgery within a vertically open 0.5-T MR system. During surgery, localization of residual tumor tissue was guided by interactive, near real-time imaging. The amount of residual tumor tissue on MR images was evaluated at the point of the operation at which the neurosurgeon would have terminated the procedure under conventional conditions (first control) and again before closing the craniotomy.**

RESULTS: **Significant residual tumor (more than 10% of original tumor volume) was shown in eight patients at the first control condition. The percentage of resection varied from 26% to 100% (mean, 68%) at this time. Twelve tissue samples from seven patients were obtained in areas identified as residual tumor on MR images. In 10 cases, the neuropathologic investigation confirmed the presence of residual low-grade glioma; in two cases, the borderzone of tumor was identified. In evaluating the final sets of images, we found total resection in six cases, over 90% resection in five cases, and 85% resection in one case (mean, 96%).**

CONCLUSION: **Surgical treatment of low-grade gliomas under intraoperative MR guidance provides improved resection results with maximal patient safety.**

The management of low-grade gliomas in the cerebral hemispheres has been a controversial topic in the literature. Treatment options have included observation only, biopsy followed by observation, surgery at the time of diagnosis or at the time of progression, radiation, and chemotherapy. Prognostic factors include age, histologic grade, tumor volume and extent of resection, preoperative neurologic status, and duration of symptoms before surgery (1–3). Nevertheless, there is now a consensus that recurrence with malignant transformation to high-grade glioma represents the major cause of mortality in these patients. Therefore, the aim of any therapy is to prevent or delay the development of a more anaplastic tumor. Recent studies have shown that surgical resection of low-grade gliomas can decrease the rate of recurrence and increase the time to tumor progression (2, 4). Additionally, it has been shown that a greater percentage of resection and a smaller volume of postoperative residual disease convey a significant advantage to the patient (1, 2, 5, 6).

The use of intraoperative sonography and electrophysiological monitoring, CT- or MR-guided stereotactic localization, frameless neuronavigational technique, and intraoperative MR imaging have facilitated resection of intracerebral lesions (7–17). The main advantages of intraoperative MR imaging are the optimal image quality (for detection of small tumor areas) and the provision of updated images (that reflect intraoperative anatomic changes) (7, 11, 12, 18–23). Hence, intraoperative MR imaging may become the imaging technique of choice for the resection of gliomas. The purpose of this study was to determine the effectiveness of intraoperative MR guidance in achieving gross-total resection of supratentorial low-grade gliomas.

Received February 4, 2000; accepted after revision May 26.

From the Departments of Diagnostic Radiology (J.P.S., T.S., F.S., J.D., S.L., T.K.), Neurosurgery (C.T., V.S.), Neuropathology (S.K., R.S.), and Anesthesiology and Intensive Care Medicine (L.S., M.L.), University of Leipzig, Germany.

Supported in part by General Electric Medical Systems, Milwaukee, WI.

Address reprint requests to Dr. Jens-Peter Schneider, Department of Diagnostic Radiology, University of Leipzig, Liebigstr. 20a, 04103 Leipzig, Germany.

Methods

All craniotomies and tumor resections in this study were carried out within a 0.5-T superconducting MR system (Signa

FIG 1. Intraoperative MR imaging environment.

A, The patient is positioned in the magnet by using the side entry of the table. The neurosurgeon can stand behind the head of the patient by using an MR-compatible microscope (*white arrow*). The assisting nurse and the surgical instrumentation table are located behind the neurosurgeon. *Black arrow* indicates in-bore monitor.

B, The Flashpoint Position Encoder (*open arrow*) with the three light-emitting diodes (*asterisks*) in situ. The MR Track Pointer (*long thin arrow*) is mounted on the Flashpoint Position Encoder.

SP/i, General Electric Medical Systems, Milwaukee, WI) (7, 11, 12, 18, 19). The surgeon can stand throughout the whole procedure in a vertical gap of 58 cm within the magnet. The patient is placed on a table that can be advanced through the bore of the magnet or through the separated partitions of the magnet (Fig 1). Imaging and surgical access to the patient without any movement of the table are possible at any time during the operation. The images can be simultaneously viewed by the surgeon on in-bore monitors and by the radiologist at the console placed in the control room.

Equipment

The following MR-compatible anesthesiologic equipment and neurosurgical instruments and tools were used (7, 11, 12): patient and gas monitor (MR Equipment, Bay Shore, NY); ventilator (Siemens, Erlangen, Germany); intraoperative microscope (Studer Medical Engineering, Rheinfall, Switzerland); bipolar electrocautery system (Erbe, Germany); ultrasonic aspirator (Elekta, Sweden); and resection instruments (Aesculap, San Francisco, CA and Codmann, Randolph, MA).

A flexible double-loop RF surface coil was fixed to the patient's head with consideration given to both the image quality required for the procedure and access to the lesion by the neurosurgeon (22). Special coil and magnet drapes guaranteed a sterile operating field.

Patients

Twelve patients (six women and six men) aged 20 to 63 years (mean age, 37 years) underwent craniotomy for tumor resection within the intraoperative MR unit between November 1997 and August 1999. Permission from the Human Studies Ethics Committee of the hospital and informed consent from the patients were obtained in every case before initiating the study.

In all cases, the preoperative clinical data and MR imaging findings were consistent with the putative diagnosis of low-grade glioma. Ten of 12 patients suffered from seizures, one patient had a defect in the field of vision, and two patients had unilateral latent hemiparesis or paresthesia. Preoperative MR imaging was performed using a 1.5-T MR unit. In nine of 12 cases, we saw a hyperintense lesion on T2-weighted images with a hypointense signal on T1-weighted images without contrast enhancement after a standard intravenous injection of gadopentetate dimeglumine. Surrounding edema (24) was present in two of 12 patients (cases 6 and 8). Only in two patients (cases 5 and 8) was an irregularly shaped contrast-enhancing nodular part of the tumor detectable. In these patients, either the tissue structure (dysembryoblastic neuroepithelial tumor, case 5) or previous therapy (resection of a WHO grade II astrocytoma and postoperative radiation 10 years earlier, case 8) was responsible for disruption of the blood-brain barrier.

Imaging Protocols

Imaging sequences are listed in Table 1. Fast spin-echo sequences, spin-echo sequences, and 3D gradient-echo sequences were used to obtain information about tumor location and residual tumor tissue. The high spatial resolution was necessary to localize the boundary of the lesions and to carry out an exact volumetric measurement of the tumor. In 10 patients, exclusively T2-weighted sequences were used for tumor localization and detection of residual tumor. Additional T1-weighted sequences were only used in cases of enhancing tumors (patients 5 and 8). In these two patients the aim was to remove the areas with disrupted blood-brain barrier to exclude foci of anaplastic dedifferentiation.

To permit interactive selection of the imaging plane, a special tracking system (Flashpoint Position Encoder, Image Guided Technologies, Boulder, CO) with three light-emitting diodes was integrated within the scanner (18). An MR Track Pointer (Daum, Schwerin, Germany) can be combined with the interactive device to improve the correlation between the surgical field and the MR images (25). This instrument (diameter, 3 mm; length, 100 or 150 mm) can be filled with a sodium chloride solution (0.9%) as well as with a solution of gadopentetate dimeglumine (1%). The interactively guided single-slice sequences (3 to 4 seconds per image) were used to plan access to the lesion before craniotomy and corticotomy (Fig 2). This continuous imaging mode was also used to detect small remnants of tumor tissue in the bed of resection that looked questionable on multislice images.

Procedure

Preparation included administering a general anesthetic, positioning the patient, attaching the flexible RF coil, and preparing and draping the surgical field. The lesion was localized using T2-weighted single-shot fast spin-echo or T1-weighted fast multiplanar spoiled gradient-echo sequences in combination with the integrated tracking device and the MR Track Pointer (Table 1 and Fig 2, top row). In cases of partially enhancing lesions, contrast material was administered intravenously (0.1 mmol/kg body weight). Interactively guided images were again obtained after the craniotomy to plan the dural

Table 1: Imaging protocol

	Sequence	TR/TE	Flip Angle (°)	Echo Train Length	FOV (cm × cm)	Matrix	Slice Thickness (mm)	Time (min)
Multislice for target localization, intraoperative resection control, and detection of residual tumor tissue*	2D, T2, FSE	2500/95	90	8	24 × 18	192 × 256	4–7	2:20–3:05
	3D, T1, FSPGR	26.8/3	15	· · ·	24 × 18	160 × 256	2–3	2:10–3:17
	2D, T1, SE	440/17	90	· · ·	24 × 18	192 × 256	4–7	05:56
Single-slice interactive for planning craniotomy, planning resection margins before dural opening, and detecting residual tumor tissue†	2D, T1, FMPSPGR	24–30/8–9	45	· · ·	24 × 24	128 × 256	10	0:04
	2D, T2, SSFSE	3102/108	90	· · ·	24 × 24	128 × 256	10	0:03

Note.—FSE indicates fast spin-echo; FSPGR, fast spoiled gradient-echo; SE, spin-echo; FMPSPGR, fast multiplanar spoiled gradient-echo; SSFSE, single-shot fast spin-echo.

* Multislice sequences (higher spatial resolution, smaller slice thickness) were used to obtain a 3D impression of the lesion, to determine its relationship to boundary structures, to detect residual tumor tissue, and to carry out the tumor volume measurement.

† Single-slice sequences were used in the continuous imaging mode in combination with the scan plan tracking system Flashpoint Position Encoder and the MR Track Pointer for interactive imaging to localize the lesion or residual tumor tissue seen on previously obtained multislice sequences.

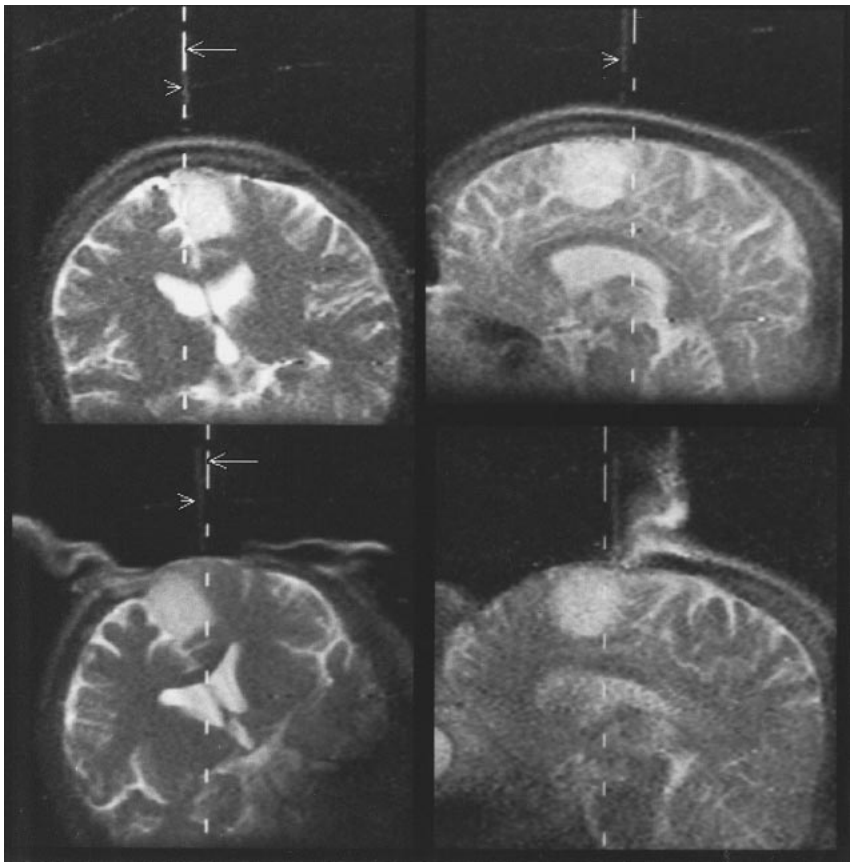

FIG 2. Patient 2 (astrocytoma, WHO grade II).

Top left and *top right,* The Flashpoint Position Encoder is used to localize the borders of the tumor in projection onto the skull before craniotomy. The *dotted lines* (*arrows*) mark the calculated actual position of the hand-held device. Additionally, an MR Track Pointer (*arrowheads*) mounted on the hand-held device is used. On T2-weighted single-shot fast spin-echo sequences, the instrument, filled with a sodium chloride solution, is displayed with high signal intensity. The sagittal view (*top right*) shows a slight deviation between the calculated and imaged positions caused by a short delay between image update (every 3 seconds) and optical tracking update (four per second).

Bottom left and *bottom right,* After craniotomy, this approach is used again to define the borders of the tumor in projection to the dura.

opening (Fig 2, bottom row). Before corticotomy, a data set of T2-weighted multislice images (in patients 5 and 8, additional T1-weighted images) with high resolution were acquired in at least two perpendicular planes. These images were used to carry out the first determination of tumor volume (Fig 3). In most cases (10/12) the T2-weighted abnormalities on the fast spin-echo images were used to define the boundary of resection. Only in two patients who had contrast enhancement of the lesion (patients 5 and 8) was the resection guided by both T1- and T2-weighted images (fast spin-echo/spin-echo or 3D fast spoiled gradient-echo).

At the point at which the surgeon considered the resection complete (as determined by inspection of the operating field with the microscope), we repeated the high-resolution T2-weighted multislice imaging sequence (in patients 5 and 8, additional T1-weighted sequences). We used the same parameters to compare the volume of tumor tissue seen preoperatively with that seen at this point of the operation. Areas of tissue that were abnormal on the multislice MR images (Figs 4 and 5) were localized in the bed of resection by using interactive MR guidance in combination with the Flashpoint system and the MR-visible Track Pointer (Figs 4 and 5). Tissue with abnormal imaging characteristics was resected when this could be accomplished safely (Figs 3–6). In patients 5 and 8, the information obtained from the T1-weighted images was used to achieve a complete resection, especially in areas with disrupted blood-brain barrier, to exclude anaplastic dedifferentiation. As a rule, an ultrasonic aspirator (Elekta) was used to

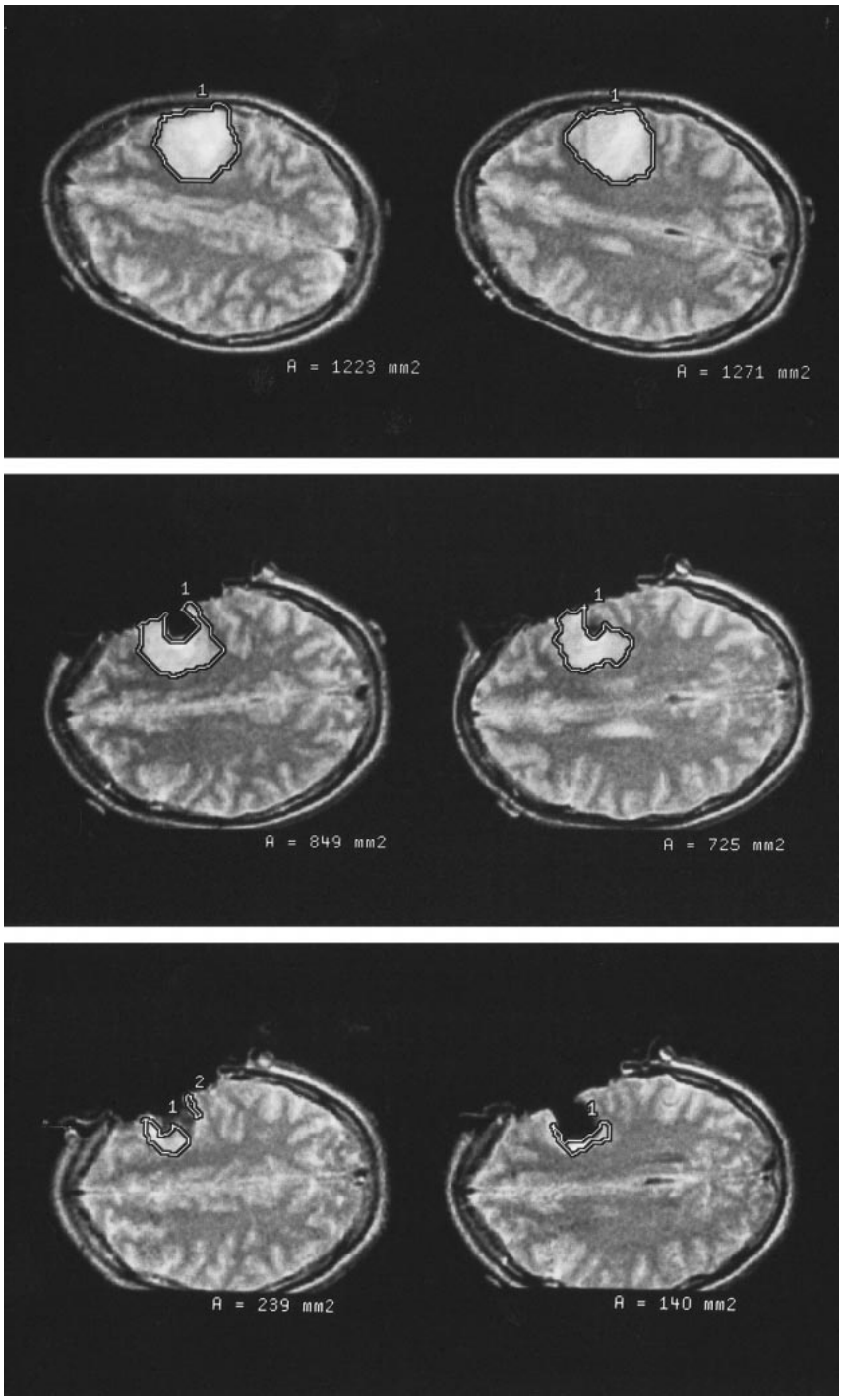

FIG 3. Patient 9 (astrocytoma, WHO grade II).

Top left and *top right,* T2-weighted axial fast spin-echo images were used to determine the tumor area before resection.

Middle left and *middle right,* Comparable slices obtained at the point at which the neurosurgeon considered the resection to be complete (first control) were used to calculate the residual tumor volume.

Bottom left and *bottom right,* T2-weighted images at the same position were used to measure very small areas of residual tumor tissue at the end of the operation before closing the craniotomy.

remove the tumor tissue. Tissue samples from areas suggestive of residual tumor on MR images were collected. These additional samples were sent to the neuropathology laboratory separately. Multislice and multiplanar MR images were obtained once again at the end of resection before and after closure of the craniotomy (Figs 3–6).

Determination of Tumor Volume

Tumor volume was ascertained in every patient three times with comparable T2-weighted fast spin-echo techniques using the same sequence, slice parameters, and scan plane: 1) before craniotomy and/or corticotomy (Fig 3, top row); 2) at the point at which the resection was considered complete by inspection of the operating field (Fig 3, middle row); and 3) at the end of the surgical procedure, before closing the craniotomy (Fig 3, bottom row).

The tumor area in each slice was measured using Signa SP/i software. On the basis of these data we calculated the volume of tissue suggestive of tumor with consideration given to thickness and gap between slices:

$$V = (A_1 + A_2 + \ldots A_n) \times (d_s + d_g\,[n-1] / n)$$

where V = volume, $A_{1\ldots n}$ = area of slices as determined by using Signa SP/i software (trace, ROI), n = number of slices, d_s = thickness of slices, and d_g = thickness of gap between the slices.

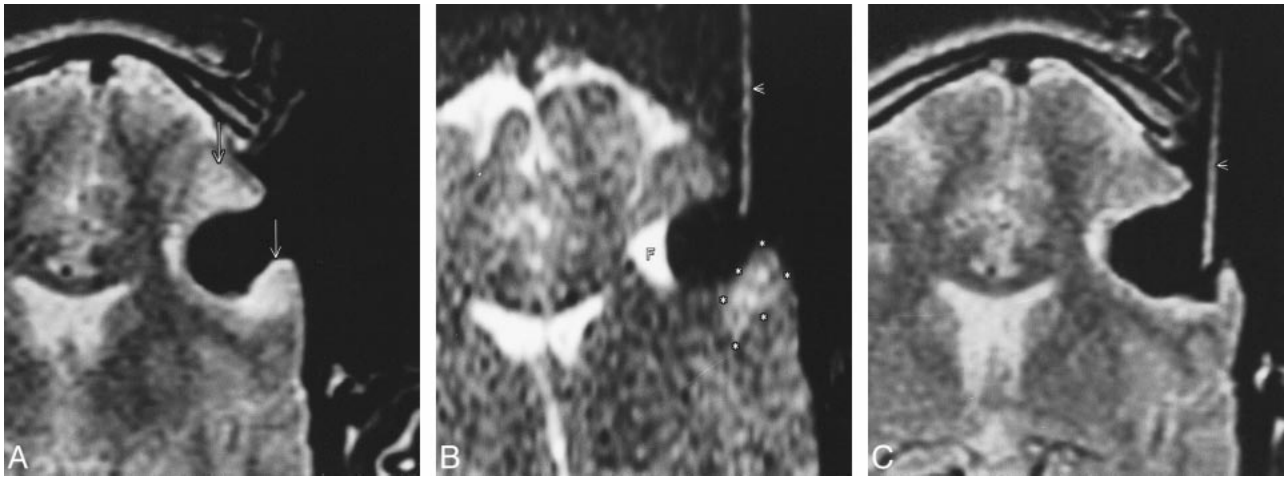

FIG 4. Patient 10 (astrocytoma, WHO grade II).

A, First control at the point at which the resection was considered complete by the neurosurgeon. T2-weighted fast spin-echo image shows two hyperintense areas suspicious for tumor (*arrows*) at the border of resection.

B, Using the interactive scan mode (T2-weighted single-shot fast spin-echo, 3 seconds per image) and the MR Track Pointer (*arrowhead*) filled with sodium chloride solution, one lesion is marked (*asterisks*). Fluid (*F*) is at the bottom of the resection cavity while the patient is lying on the right side.

C, The last control (T2-weighted fast spin-echo image) shows complete removal of all tumor-suspicious tissue. There is no surgically induced edema evident in the bed of resection.

Results

No technical difficulties or intraoperative complications were encountered in any of the 12 procedures. The diagnosis of primary low-grade glial tumor (one dysembryoblastic neuroepithelial tumor, six WHO grade II astrocytomas, three WHO grade II oligodendrogliomas, and two WHO grade II mixed oligoastrocytomas) was confirmed in all 12 cases by neuropathologic investigation of specimens obtained from representative parts of the tumor. We selected patients with primary glial lesions grade I or II (according to the WHO classification) from a prospective study population of 79 patients who underwent resection of brain tumors under MR guidance using the same procedure and imaging protocol as prescribed above.

Patient Outcome

Postoperatively, eight patients had no functional neurologic deficit. In one patient (case 8), there was no change of a preexisting left-sided hemiparesis. In two patients who underwent resections marginally involving the language cortex, we saw mild dysphasia that resolved after 3 months. In one patient with a large precentral tumor, a discrete paresis of the right hand was still evident 3 months after surgery.

Procedure

Exact neurosurgical access planning was carried out in every patient before craniotomy and corticotomy by using the interactive guidance system in a near real-time imaging mode (Fig 2). In seven patients with subcortical lesions, observation after dural opening revealed a normal brain surface. In these patients, the corticotomy was guided by the information obtained from the near real-time MR images.

Elapsed time between dural opening and the first control condition ranged from 113 to 261 minutes (mean, 172 minutes). In 11 of 12 patients, residual tumor tissue was detected on the MR images, and the operation was continued and imaging was used to localize the residual tumor tissue. In all, we performed 10 to 31 (mean, 23) multislice sequences and three to five (mean, four) interactively guided single-slice sequences per patient. When multislice data were required (range, 22 to 92 minutes; mean, 56 minutes per patient), surgery was stopped. During the interactively guided sequences (range, 9 to 51 minutes; mean, 29 minutes per patient), the operation continued. The total operation time ranged from 169 to 346 minutes (mean, 281 minutes).

Determination of Tumor Volume

When comparing tumor volume before resection and at the point at which the neurosurgeon would otherwise have terminated the operation (first control condition), significant residual tumor tissue (more than 10% of the original tumor volume) was seen on MR images in eight patients. In four patients, no or almost no tumor-suspicious tissue was seen when the resection was considered complete by the neurosurgeon. In two of these cases, the surgeon was able to differentiate tumor clearly from surrounding normal brain by inspection before starting the corticotomy. In two patients with an almost complete resection, and in all patients ($n = 8$) with incomplete results at this point in the surgery, the brain surface was inconspicuous after craniotomy and dural opening. In summary, at this

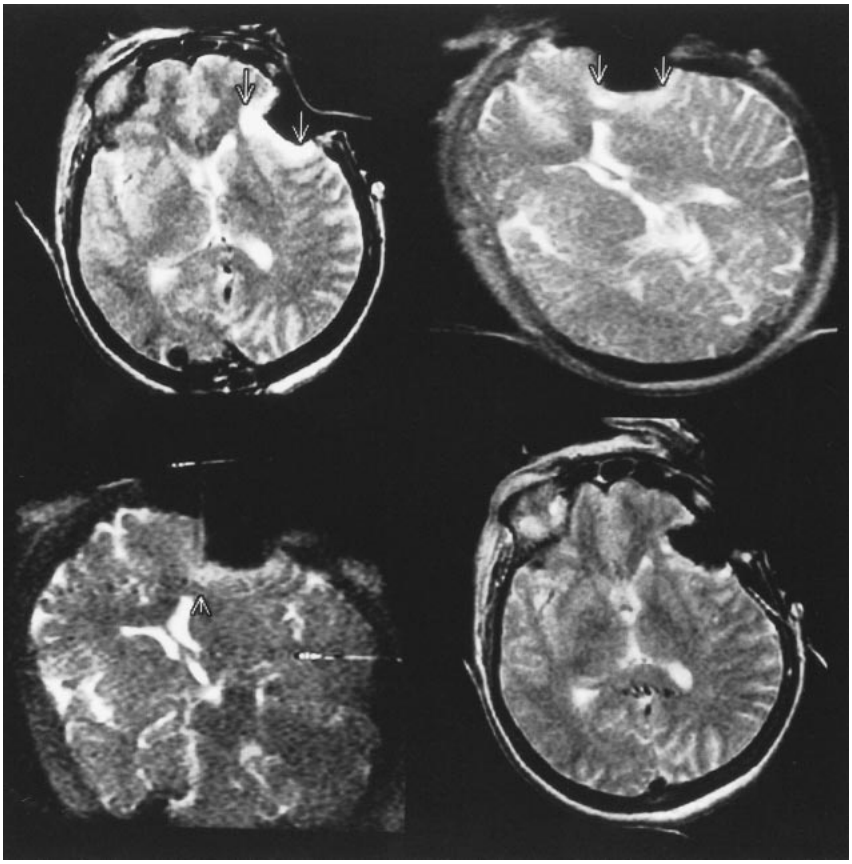

FIG 5. Patient 4 (oligodendroglioma, WHO grade II).

Top left, The first control image (T2-weighted fast spin-echo) shows hyperintense tumor-suspicious tissue (*arrows*) in the bed of resection.

Top right and *bottom left,* Abnormalities are also seen on the interactively guided single-shot fast spin-echo images (*arrows*). The MR Track Pointer is used to localize the suspicious area (*arrowhead*).

Bottom right, Before closure of the craniotomy, T2-weighted fast spin-echo image shows the final result of the resection. The tumor-suspicious tissue was reduced; nevertheless, some nodular areas are still suggestive of residual tumor. Because of the proximity of this region to the language cortex, the resection was stopped at this point. The patient had no postoperative neurologic deficit.

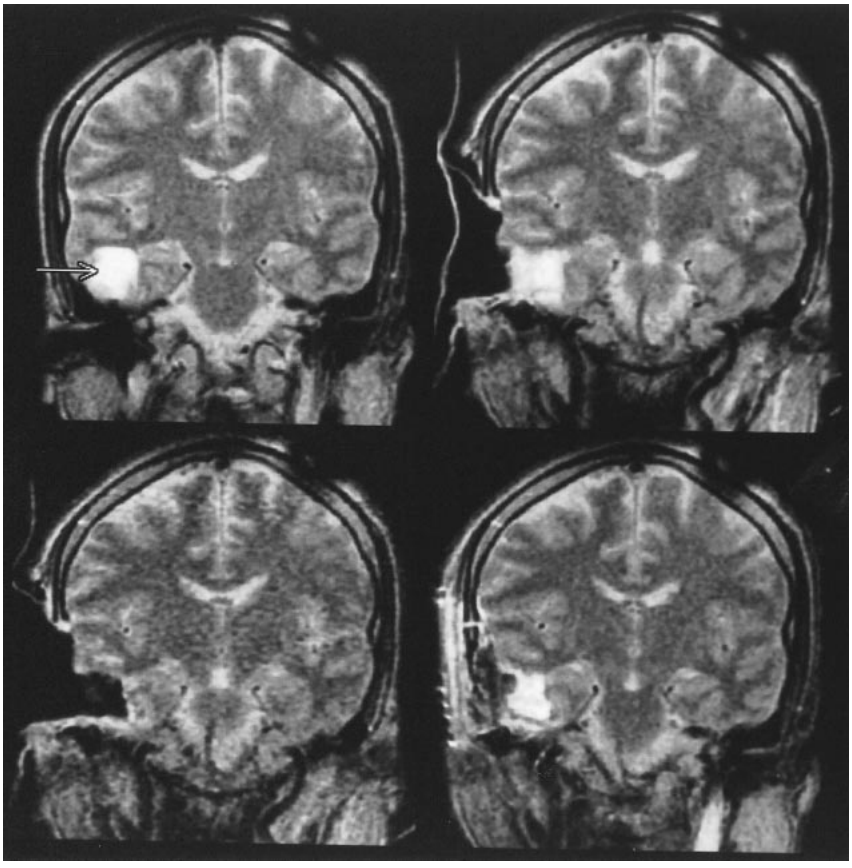

FIG 6. Patient 1 (astrocytoma, WHO grade II).

Top left, T2-weighted fast spin-echo image before craniotomy shows high signal intensity of the temporal astrocytoma (*arrow*).

Top right, T2-weighted fast spin-echo image after corticotomy for surgical access to the tumor.

Bottom left, T2-weighted fast spin-echo image at the point at which resection was considered complete by the neurosurgeon and by the radiologist reveals no residual tumor at this slice.

Bottom right, After closure of the craniotomy, the bed of resection is displayed with high signal intensity, probably caused by a mixture of blood, CSF, saline, and hemostatic material.

Table 2: Tumor volume at different points of the operation

Patient No.	Histologic Diagnosis	Preoperative Tumor Volume (mm^3)	First Control Condition Tumor Volume (mm^3)	Residual Tumor Tissue (%)	End of Resection Tumor Volume (mm^3)	Residual Tumor Tissue (%)
1	Astrocytoma, WHO II	9,000	0	0	0	0
2	Oligodendroglioma, WHO II	10,200	400	4	0	0
3	Astrocytoma, WHO II	22,300	8,400	38	0	0
4	Oligodendroglioma, WHO II	25,400	10,600	42	1,400	5.5
5	Dysembryoblastic neuroepithelial tumor, WHO I	39,500	1,600	4	0	0
6	Oligodendroglioma, WHO II	78,600	35,800	46	12,200	15.5
7	Mixed oligoastrocytoma, WHO II	48,100	35,400	74	3,500	7.3
8	Astrocytoma, WHO II (first recurrence)	32,500	3,100	9	2,000	6.2
9	Astrocytoma, WHO II	8,000	4,200	52	700	8.8
10	Astrocytoma, WHO II	25,400	14,000	55	0	0
11	Astrocytoma, WHO II	748	170	23	0	0
12	Mixed oligoastrocytoma, WHO II	23,200	8,500	36	1,900	8.2
				mean = 32		mean = 4.3

Note.—Preoperative tumor volume is that before craniotomy or corticotomy, first control condition is that at the point at which the resection was cons idered complete by inspection of the operating field, and end of resection was before closing the craniotomy.

FIG 7. Volume of tumor/residual tumor detected on MR images in all 12 patients at three different points of resection: 1) preoperatively (before craniotomy/corticotomy), 2) at the point of first control condition (when resection was considered complete by inspection of the operative field), and 3) at the conclusion of surgery (before closing craniotomy).

first point of control, we saw residual tumor tissue at a rate of 0% to 74% (mean, 32%) (Table 2 and Fig 7).

At the end of the procedure, before closing the craniotomy, no residual tumor was observed in six of 12 cases, either by visual microscopic inspection or on MR images. In six patients with tumors located in or near eloquent brain areas (motor or language cortex) we saw residual tumor tissue at a rate of 5.5% to 15.5% (mean, 4.3%) (Table 2 and Fig 7). In all, total (100%) resection was achieved in six of 12 cases, greater than 90% resection in five cases, and 85% resection in only one case (mean percentage of resection, 95.7%).

Histologic Examination of MR-suggestive Tumor Remnants

Tissue areas still requiring resection could be located in the surgical field by using the updated information provided by multislice MR imaging and the interactive scanning mode (Figs 4 and 5). Twelve additional tissue samples identified as residual tumor on MR images were removed in seven patients. In two patients, the soft tissue with suspected tumor was sucked out and not collected for investigation. In 10 of the 12 samples, the neuropathologic examination confirmed the presence of low-grade glioma. Only two samples showed borderzone changes of an otherwise unspecified pathologic process.

Discussion

The treatment regime that should be offered to patients with low-grade astrocytomas and other low-grade glial tumors is a subject of controversy. The results of different studies regarding survival time and 5-year survival rates clearly indicate that low-grade gliomas cannot be considered benign tumors, as these patients die of tumor progression or

recurrence, with a clear tendency toward anaplastic change (1–5, 26–31). Tumor detection at a young age, long-standing preoperative symptoms, small tumor size, and gross-total resection have all been associated with longer survival (1–3, 5, 26, 31, 32). Progress in MR imaging has allowed earlier detection of these tumors in recent years, affording greater opportunity for therapeutic intervention before the evolution of anaplastic dedifferentiation.

Two main problems are associated with the surgical treatment of low-grade gliomas. The first is the risk of causing a significant neurologic deficit if tumors are located near eloquent brain areas. Second, a true gross-total resection based on direct visualization or use of an operative microscope is often not possible. Hence, there is a tendency for surgeons to perform incomplete resections, especially in the vicinity of the eloquent cortex. One series (4) reported a mean resection rate of 76%, and another (1) reported 32% total resections and 68% subtotal resections.

MR imaging seems to be the intraoperative imaging technique of choice for gliomas, as it can provide updated information during the intervention (7–9, 11, 12, 17, 19–22). Low-grade gliomas (especially astrocytomas) are nonenhancing lesions that generally have well-defined margins on MR images. In our small group we found such a characteristic in nine of 12 patients. Moreover, intraoperative MR guidance eliminates some of the problems caused by the use of preoperative imaging in frame-based or frameless neuronavigational systems (15, 16, 32–34). All anatomic changes that occur during the operation (eg, brain shifts) can be detected and adjustments made during the procedure. Intraoperative MR imaging provides a view of deeper structures before superficial tissue has been removed and allows interactive, near real-time guidance during some steps of the resection procedure (7, 20, 22).

This study is one of the first to assess the value of intraoperative MR imaging in the treatment of low-grade gliomas. We determined the volume of residual tumor tissue at the point at which the neurosurgeon would have terminated the operation without intraoperative imaging. The mean percentage of resection at this stage of the operation was 68%. Among the 12 patients in the series, in four patients, 90% to 100% of the tumor volume was removed (gross-total resection), whereas in eight patients, only a subtotal resection was attained at this time.

Several factors have to be considered as possible causes of bias in our study design. The neurosurgeon had access to preoperative imaging studies, including interactively guided, near real-time images performed before corticotomy, and may have been influenced by knowing the exact location of the tumor. On the other hand, the surgeon, perhaps even subconsciously, may have decided to terminate the resection early to be safe. We speculate that these two factors may have negated each other, as the percentage of tumor resection at this step of the operation was comparable to that reported by others using conventional methods (1, 4).

The application of intraoperative, interactive MR imaging permits identification of the precise location of residual tumor tissue. Using near real-time MR imaging in a continuous imaging mode in combination with an integrated optical tracking system, we performed resection of the suspicious areas under interactive MR guidance. The neuropathologic analysis of additional specimens revealed tumor tissue in 10 of 12 cases and a borderzone in two of 12 cases, thus demonstrating the feasibility of an accurate anatomic identification of tumor remnants in the bed of resection. By the end of the surgical procedure, we achieved an average resection rate of 96%.

In recent years, a number of groups have observed a major correlation between the extent of glioma resection and prognosis for survival (1, 4, 5, 26, 31). This type of tumor in particular seems to be an excellent candidate for intraoperative MR imaging. In most cases, there is a clear tumor margin on T2-weighted images. In such instances, administration of a contrast agent is not necessary. Hence, problems with surgically induced contrast enhancement do not occur (8, 23, 35). In two patients (cases 5 and 8), we observed only a contrast-enhancing, bandlike area about 1-mm thick at the resection margin after complete removal of the nodular enhancing parts of the lesion. In our experience, the concern about extensive ''finger-shaped'' areas of increased signal intensity on T2-weighted images in the bed of resection, postulated to be surgically induced edema, is not justified (8, 24). Despite the use of electrocoagulation and an ultrasonic aspirator for resection, only a very small abnormality was evident on T2-weighted images when good hemostasis in the bed of resection was achieved (Figs 3–6). Contrary to other reports (8), we could not find neurosurgically induced edema exceeding the described 1- to 3-mm-thick T2-weighted hyperintense borderline at the resection margin (35). In this borderzone of the surgical cavity, we found a similar linear 1- to 3-mm-thick area of enhancement with a maximum intensity 15 minutes after contrast application (35). In our opinion, the strong linear appearance of these borderzone changes seen on T2- and T1-weighted images may be attributable to surgically induced microcontusions in the bed of resection, resulting in disturbances of the blood-brain barrier and leakage of microvessels with interstitial serum content and edema. The diagnosis of residual tumor tissue was made on the basis of observed nodular T2-weighted hyperintense structures in the bed of resection when the surgical cavity was proved to be free of hemostyptic materials and fluid. The results of neuropathologic examination of 12 additional tissue samples resected from small areas suspected to harbor tumor confirmed the diagnoses of tumor remnants in 10 cases. The remaining two specimens

showed borderzone changes that are common in tissue surrounding tumor.

After wound closure, imaging characteristics that simulated the appearance of removed tumor were detected in every case in the bed of resection (Fig 6). These were probably caused by a combination of CSF, blood, sodium chloride solution, and hemostatic material. At this point in the procedure, residual tumor cannot be differentiated from postoperative changes; however, imaging at the conclusion of surgery can be very helpful in detecting early postoperative complications, such as hemorrhage (19). We did not observe such a complication in our small group.

All data presented in this study were obtained from MR images only and cannot imply a true histologically complete resection. As noted in previous reports, it is well known that primary neoplasms within the brain can extend well beyond signal abnormalities on MR studies. However, the majority of the lesions we combined under the term low-grade glioma, according to the WHO classification system, consisted of parenchyma diffusely infiltrated with isolated tumor cells (26, 32). MR images can misleadingly display these lesions as clearly defined, but tumor cells can be found outside the MR-visible border of the tumor. Nevertheless, in all these patients with several types of glial brain tumor (WHO grades I or II), the extent of resection seemed to be the only prognostic factor that could be influenced by therapy (32). Additionally, the aim of the study was to evaluate the effectiveness of intraoperative MR imaging in gross-total resections based on MR imaging characteristics in comparison with the results of conventional neurosurgical methods. It was not our intention to prove the accuracy or extent of the resection histologically, because there is no accepted method for this in vivo.

Our preliminary experience with intraoperative MR guidance in the surgical treatment of low-grade gliomas is encouraging. Beyond the possibility of being able to plan interactively the surgical approach with great certainty before craniotomy and corticotomy, this technology substantially improves the precision of resection as well. One remaining problem is that accurate anatomic identification of the tumor does not fully protect against a postoperative neurologic deficit caused by partial resection of eloquent areas of the brain within or near the tumor. To solve this problem, an electrocorticographic system for use with intraoperative MR imaging could be a helpful instrument (7).

Because of the short follow-up period of these patients, it is too early to make definitive statements as to long-term outcome. For the same reason, any possible benefits in regard to survival rates and a cost analysis of length of survival and quality of life cannot be ascertained at this time. We propose that such data, gained by multisite trials, should be collected worldwide to characterize the future role of intraoperative MR imaging in the treatment of low-grade gliomas.

Conclusion

Survival of patients with low-grade gliomas correlates with the extent of resection. However, these tumors are difficult to distinguish intraoperatively from normal brain tissue, often leading to incomplete resection. To evaluate the effectiveness of intraoperative MR guidance in achieving gross-total resection, 12 patients with supratentorial low-grade glioma underwent surgery within a vertically open 0.5-T MR system. Significant residual tumor was shown on MR images in eight patients at the point during surgery when the neurosurgeon considered the procedure complete, as determined by visual inspection of the operative field. Tissue with tumor-suspicious imaging characteristics was localized and resected when this could be accomplished safely. In evaluating the final set of images, we determined that total resection was achieved in six cases, more than 90% resection in five cases, and 85% resection in one case (mean percentage of resection, 96%). The combination of optical control (directed by the neurosurgeon) and MR control (carried out by the radiologist) seems to be helpful in improving the clinical outcome of patients with low-grade gliomas.

Acknowledgments

We thank all of the technical and nursing staff of the Department of Diagnostic Radiology, especially Cathrin Voerkel, Brit Martin, and Angela Schmidt for their assistance and commitment during the last months to inaugurate interventional MRI at our hospital. Special thanks also to Erik Penner, Timo Schirmer, and Rob Newman at General Electric Medical Systems.

References

1. Philippon JH, Clemenceau SH, Fauchon FH, Foncin JF. **Supratentorial low grade astrocytomas in adults.** *Neurosurgery* 1993; 32:554–559
2. Piepmeier J, Christopher S, Spencer D, et al. **Variations in the natural history and survival of patients with supratentorial low-grade astrocytomas.** *Neurosurgery* 1996;38:872–879
3. Laws ER, Taylor WF, Clifton MB, Okazaki H. **Neurosurgical management of low-grade astrocytoma of the cerebral hemispheres.** *J Neurosurg* 1984;61:665–673
4. Berger MS, Deliganis AV, Dobbins J, Keles GE. **The effect of extent of resection on recurrence in patients with low grade cerebral hemisphere gliomas.** *Cancer* 1994;74:1784–1791
5. Janny P, Cure H, Mohr M, et al. **Low grade supratentorial astrocytomas: management and prognostic factors.** *Cancer* 1994; 73:1937–1945
6. Healy EA, Barnes PD, Kupsky WJ, et al. **The prognostic significance of postoperative residual tumor in ependymoma.** *Neurosurgery* 1991;28:666–671
7. Martin C, Alexander EA, Wong T, Schwartz R, Jolesz F, Black PM. **Surgical treatment of low-grade gliomas in the intraoperative magnetic resonance imager.** *Internet Comm Neurosurg Focus* 1998;4:article 8
8. Knauth M, Wirtz CR, Tronnier VM, Staubert A, Kunze S, Sartor K. **Intraoperative MRI to control the extent of brain tumor surgery.** *Radiologe* 1998;38:218–224
9. Tronnier VM, Wirtz CR, Knauth M, et al. **Intraoperative diagnostic and interventional magnetic resonance imaging in neurosurgery.** *Neurosurgery* 1997;40:891–900
10. Lunsford LD, Parrish R, Albright L. **Intraoperative imaging with a therapeutic computed tomographic scanner.** *Neurosurgery* 1984;15:559–561

11. Schmidt F, Dietrich J, Schneider JP, Thiele J, Lieberenz S, Werner A, Grunder W. **Technological and logistic problems and first clinical results of an interventional 0.5-T MRI system used by various medical specialties.** *Radiologe* 1998;38:173–184
12. Schneider JP, Dietrich J, Lieberenz S, Schmidt F, et al. **Preliminary experience with interactive guided brain biopsies using a vertically opened 0.5 Tesla MR system.** *Eur Radiol* 1999;9:230–236
13. van Velthofen V, Auer LM. **Practical application of intraoperative ultrasound imaging.** *Acta Neurochir* 1990;105:5–13
14. Hammoud MA, Ligon BL, El Souki R, et al. **Use of intraoperative ultrasound for localizing tumors and determining the extent of resection: a comparative study with magnetic resonance imaging.** *J Neurosurg* 1996;84:737–741
15. Sipos EP, Tebo SA, Zinreich SJ, Long DM, Brem H. **In vivo accuracy testing and clinical experience with the ISG viewing wand.** *Neurosurgery* 1996;39:194–203
16. Tronnier VM, Wirtz CR, Knauth M, et al. **Intraoperative computer-assisted neuro-navigation in functional neurosurgery.** *Stereotact Funct Neurosurg* 1996;66:65–68
17. Steinmeier R, Fahlbusch R, Ganslandt O, et al. **Intraoperative magnetic resonance imaging with the Magnetom open scanner: concepts, neurosurgical indications, and procedures: a preliminary report.** *Neurosurgery* 1998;43:739–747
18. Schenck JF, Jolesz FA, Roemer PB, et al. **Superconducting open configuration MRI system for image-guided therapy.** *Radiology* 1995;195:805–814
19. Black PML, Moriarty T, Alexander E, et al. **Development and implementation of intraoperative magnetic resonance imaging and its neurosurgical applications.** *Neurosurgery* 1997;41:831–845
20. Seifert V, Zimmermann M, Trantakis C, et al. **Open MRI-guided neurosurgery.** *Acta Neurochir (Wien)* 1999;141:455–464
21. Kahn T, Schmidt F, Modder U. **MR imaging-guided interventions.** *Radiologe* 1999;39:741–749
22. Schwartz RB, Hsu L, Wong TZ, et al. **Intraoperative MR imaging guidance for intracranial neurosurgery: experience with the first 200 cases.** *Radiology* 1999;211:477–488
23. Knauth M, Wirtz CR, Tronnier VM, et al. **Intraoperative MR imaging increases the extent of tumor resection in patients with high-grade gliomas.** *AJNR Am J Neuroradiol* 1999;20:1642–1646
24. Kahn T, Bettag M, Ulrich F, Schwarzmaier HJ, Schober R, Furst G, Modder U. **MRI-guided laser-induced interstitial thermotherapy of cerebral neoplasms.** *J Comput Assist Tomogr* 1994;18:519–532
25. Schulz T, Schneider JP, Winkel A, et al. **"MR-Track-Pointer": a reusable instrument for localisation during interventions.** *Fortschr Rontgenstr* 1999;171:244–248
26. Berger MS. **Role of surgery in diagnosis and management.** In: Apuzzo MLJ, ed. **Benign Cerebral Glioma.** Park Ridge, IL: AANS,1995:293–307
27. Mc Cormack BM, Miller DC, Budzilovich GN, Voorhees GJ, Ransohoff J. **Treatment and survival of low-grade astrocytoma in adults, 1977–1988.** *Neurosurgery* 1992;31:636–642
28. Shaw E, Earle J, Scheithauer B, et al. **Postoperative radiation for supratentorial low-grade gliomas.** *Int J Radiat Oncol Biol Phys* 1987;13:148
29. Vertosick FT, Selker RG, Arewa VC. **Survival of patients with well-differentiated astrocytomas diagnosed in the era of computed tomography.** *Neurosurgery* 1991;28:496–501
30. Salcman M. **Radical surgery for low grade glioma.** *Clin Neurosurg* 1988;36:353–366
31. Nicolato A, Gerosa MA, Fina P, et al. **Prognostic factors in low-grade supratentorial astrocytomas: a uni- multivariate statistical analysis in 76 surgically treated patients.** *Surg Neurol* 1995;44:208–223
32. Kelly PJ. **CT/MRI-based computer-assisted volumetric stereotactic resection of intracranial lesions.** In: Schmidek HH, Sweet WH, eds. Operative Neurosurgical Techniques. 3rd ed. Philadelphia: Saunders;1995:619–635
33. Gallowa RL, Maciunas RJ, Latimer JW. **The accuracies of four stereotactic frame systems: an independent assessment.** *Biomed Instrum Technol* 1991;25:457–460
34. Nauta HJW. **Error assessment during "image-guided" and "imaging interactive" stereotactic surgery.** *Comput Med Imaging Graph* 1994;18:279–287
35. Dietrich J, Schneider JP, Schulz T, Seifert V, Trantakis C, Kellermann S. **Intra-operative appearance of the resection area in brain tumor operations in an open 0.5T MRT.** *Radiologe* 1998;38:935–942